IEEE Access
Multidisciplinary ⋮ Rapid Review ⋮ Open Access Journal

Received 13 May 2023, accepted 4 June 2023, date of publication 9 June 2023, date of current version 19 June 2023.

Digital Object Identifier 10.1109/ACCESS.2023.3284390

RESEARCH ARTICLE

Artificial Rabbits Optimizer With Machine Learning Based Emergency Department Monitoring and Medical Data Classification at KSA Hospitals

LUBNA A. ALHARBI
Department of Computer Science, Faculty of Computers and Information Technology, University of Tabuk, Tabuk 71491, Saudi Arabia
e-mail: lualharbi@ut.edu.sa

This work was supported by the Deanship of Scientific Research (DSR), University of Tabuk, Saudi Arabia, under Grant S-1443-0273.

ABSTRACT The Emergency Departments (EDs) in health centres located in the main areas of Saudi Arabia have heavy patient inflow because of the pandemic, viral infections, and even on some special occasions like Umrah or Hajj, where pilgrims who travel from one place to another with serious disorders. Other than the EDs, it was important to observe the patient's activities from ED to other wards in the region or the hospital to track the spread of viral diseases. In this case, deep learning (DL) and machine learning (ML) methods have been used to track the target audience and classify the data into many classes. With this motivation, this study develops an artificial rabbit optimization with a machine learning-based healthcare data classification (AROML-HDC) technique for EDs. The AROML-HDC technique monitors and tracks the patient visit data, treatment given, and length of stay (LOS). In addition, the AROML-HDC technique designs an effective ARO algorithm for the optimal selection of feature subsets. Next, the class-specific cost regulation extreme learning machine (CSCR-ELM) classifier is applied for effective medical data classification. Finally, the grasshopper optimization algorithm (GOA) was used to adjust the parameters related to the CSCR-ELM classifier. The experimental outcome of the AROML-HDC approach is tested on the benchmark Cleveland dataset and the Statlog dataset comprising 297 and 270 samples, respectively. The simulation results signify the improved performance of the AROML-HDC technique over other recent methods with maximum accuracy of 93.22% and 94.05% Cleveland dataset and the Statlog dataset, respectively.

INDEX TERMS Medical data classification, emergency departments, KSA hospitals, feature selection, machine learning.

I. INTRODUCTION

Recently, the healthcare field is generating data from a lot of patients and facilities. By using this data, clinicians can easily anticipate better techniques for treatment and boost the medical field [1]. One significant use of the python structure encourages computing facilities to extract useful insights from the data over the healthcare domain. Disease diagnosis is determining the disease through symptoms of persons [2]. The challenging issue in the diagnosis is some signs and symptoms were non-specific. Machine learning (ML) helps to forecast the disease diagnosis depending on the prior training data. Several scientists have made different ML techniques to work well to diagnose different diseases [3]. ML presents the capability for machines to learn without being specifically programmed. Evolving a model by ML techniques can forecast an initial-stage disease diagnosis and render solutions. Effective treatment and initial diagnosis are the optimal way to reduce death rates [4]. Hence, many clinical scientists have adopted new methods for predicting diseases depending on ML techniques.

The associate editor coordinating the review of this manuscript and approving it for publication was Xiong Luo.

Artificial intelligence (AI) is defined as human intelligence executed by machines [5]. In computer science, it is considered as the capability of machines to emulate intellectual behaviour by itself, utilizing ML [6]. In medicine, AI applications are growing rapidly. In the medical field, AI is the use of automated diagnosis and the treatment of victims who need care. Generally, ML is classified as unsupervised (which deals with clustering of various groups for specific interventions) or supervised (composed of output parameters that are estimated from input variables) [7]. ML can determine complex methods, expose innovative ideas to doctors, and extract medical knowledge. In medical practice, ML prediction algorithms can point out improved rules in deciding on individual patient care. The infusion of such methods in drug prescription can offer new medical openings in pathology recognition and save clinicians [8]. The medical data quality can probably be enhanced with ML methods, save medical costs and lessen fluctuations in patient rates. Consequently, these methods are often utilized for investigating diagnostic analysis than other classical techniques [9]. Early recognition and potential treatments will be the only solution for reducing the mortality rates caused by chronic disease (CD). Thus, many medical scientists were attracted towards the innovative technologies of prediction approaches in forecasting diseases [10].

This study presents an artificial rabbit optimization with a machine learning-based healthcare data classification (AROML-HDC) technique for EDs. The presented AROML-HDC technique monitors and tracks the patient visit data, treatment given, and length of stay (LOS). In addition, the AROML-HDC technique designs an effective ARO algorithm for optimal selection of feature subsets. Next, class-specific cost regulation extreme learning machine (CSCR-ELM) classifier is applied for effective medical data classification. Finally, the grasshopper optimization algorithm (GOA) is used to adjust the parameters related to the CSCR-ELM classifier. The experimental outcome of the AROML-HDC method is tested on a benchmark healthcare dataset.

The rest of the paper is organized as follows. Section II provides the related works and section III offers the proposed model. Then, section IV gives the result analysis and section V concludes the paper.

II. RELATED WORKS

Kishor and Chakraborty [11] presented an ML-based healthcare method for accurate and early prediction of various diseases. In this study, seven ML classifier techniques like Random Forest (RF), decision tree, Naïve Bayes, adaptive boosting, K-NN, SVM, and ANN were exploited for forecasting the nine deadly diseases like hepatitis, heart disease, liver disorder, dermatology, thyroid, surgery data, spect heart and diabetics breast cancer. In [12] presented a new technique using ML (k-fold random forest) named Intelligent Multimedia Data Segregation (IMDS) technique in the fog-computing atmosphere that separates the multimedia data and the method computes total latency (computation and network transmission).

In [13], devised a new healthcare monitoring structure depends on the cloud environment and a big data analytics engine to analyse and store medical data accurately and to boost the classifier accuracy. The presented big data analytics engine depends on Bi-LSTM, data mining algorithms, and ontologies. The presented ontologies afford semantic knowledge regarding aspects and entities and their relations in the fields of blood pressure (BP) and diabetes. To forecast abnormal circumstances and side effects of drugs in patients, Bi-LSTM is used that properly categorizes the health care data. In [14], developed an IoT-based student health care monitoring approach to identify behavioural and biological changes and check student vital signs through smart health care technologies. Here, to detect the risks of students' behavioural and physiological changes, vital data are gathered through IoT gadgets and with the use of ML methods, data analysis is enacted. Samantha et al. [15] meant to design a precise technique to classify sleep phases by features of Heart Rate Variability (HRV) from an Electrocardiogram (ECG). To forecast sleep stages proportion, the sleep stages classification is applied. This sleep stage proportion data offer insight into human sleep quality. The hybridized PSO and ELM were applied to determine hidden nodes and choose features.

In [16], a general structure has been modelled for disease prediction in the field of medicine. This system has experimented through enhanced SVM-Radial bias kernel approach with less set features of Heart Disease, Chronic Kidney Disease, and Diabetes dataset, and this system has compared with other ML approaches like Random forest, SVM-Linear, Decision tree, and SVM-Polynomial in R studio. In [17], the authors have implemented various ML approaches and considered public data of healthcare saved in the cloud to construct a system which allowed remote health monitoring constructed on IoT structure and linked with cloud computing. The authors devised a structure to expose knowledge in databases, and lightening disguise patterns help in credible decision-making.

Oskvarek et al. [18] assessed and developed variation in an emergency department (ED) admission intensity measure proposed for value-based payment methods. The measure involves ED diagnosis amenable to evidence-related protocol and where admission decisions change related to physician discretion. Kadri et al. [19] introduced a DL-driven method to forecast the patient LOS in ED utilizing a GAN approach. The GAN-driven method flexibly learned appropriate data from nonlinear and linear processes without preceding assumptions on data dispersion and enhanced the forecasting accuracy. Kavitha and Ravikumar [20] devise a four-module structure containing a context-aware module (CA-M), an IoT module (IoT-M), data preprocessing module (DP-M), along with decision-making module (DM-M) to store and process several cumulative sensor datasets.

Goto et al. [21] inspect the performance of ML methods for forecasting medical outcomes and disposition in children in the ED and to compare performance with old triage methods. Nymoen et al. [22] study intends to inspect the prevalence of drug-oriented emergency department (ED) visits and related risk factors.

III. THE PROPOSED MODEL

In this study, we have presented a new AROML-HDC technique for medical data classification and monitoring in the EDs of the KSA hospitals. The presented AROML-HDC technique monitors and tracks the patient visit data, treatment given, and LOS. In addition, the AROML-HDC technique performs medical data classification via different sub-processes, namely min-max normalization, ARO-based feature subset selection, CSCR-ELM classification, and GOA-based parameter tuning. Fig. 1 represents the workflow of the AROML-HDC approach.

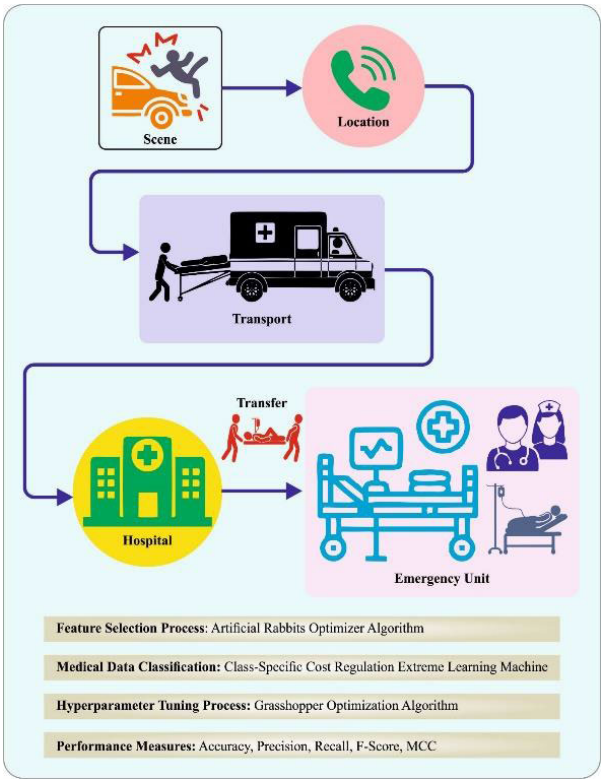

FIGURE 1. Workflow of AROML-HDC approach.

A. DATA PRE-PROCESSING

Min-max normalization [23] was broadly used to scale the data to unit variance. This can be used to compute the similarity degree in-between the points. Assume A as data that can be mapped from data range from Amin to Amax, utilizing Eq. (1):

$$A_{normalized} = \frac{A - A_{min}}{A_{max} - A_{min}} \tag{1}$$

The min-max normalization usage confirmed that the feature has been exacted to similar scales.

B. ALGORITHMIC DESIGN OF ARO-BASED FEATURE SELECTION APPROACH

The ARO algorithm is utilized in this work to choose optimal features. The survival strategy utilized by rabbits in nature draws inspiration towards the ARO technique [24]. Rabbits looking for food far from their nest is named detour foraging behaviour. It makes them burrow around their nests and arbitrarily hide to escape from the hunter and predator; this is named the random hiding behaviour. They decide to make random hiding or detour foraging relies upon the energy. Once they have lower energy, they hide randomly in the nearby burrow around their nest, and once they have sufficient or high energy, they find food at a location far from their nest (detour foraging).

1) ENERGY SHRINK (SWITCH BETWEEN EXPLOITATION AND EXPLORATION)

The rabbit decides to make either a detour foraging or random hiding. This relies on the quantity of rabbit energy. Hence the energy factor $A(t)$ can be evaluated based on Eq. (2) for stimulating which one the rabbit performs. If $A(t) \leq 1$, they perform random hiding and if $A(t) > 1$, rabbits perform detour foraging.

$$A(t) = 4\left(1 - \frac{t}{T}\right)\ln\frac{1}{r} \tag{2}$$

In Eq. (2), r refers to a number selected randomly within [0, 1].

2) DETOUR FORAGING (EXPLORATION)

Rabbit finds food far from their nest, securing their nests from predators. Eq. (3) represents that rabbits randomly find food based on the position of others.

$$\begin{aligned}\vec{p}_i(t+1) &= \vec{\chi}_i + R \times \left(\vec{x}_i(t) - \vec{\chi}_j(t)\right) \\ &\quad + round\,(0.5 \times (0.05 + r_1)) \times n_1, i, j \\ &= 1, \ldots, n \text{ and } j \neq i\end{aligned} \tag{3}$$

$$R = L \times c \tag{4}$$

$$L = (e - e^{(\frac{t-1}{T})^2} \times sin(2\pi r_2) \tag{5}$$

$$c(k) = \begin{cases} 1 \text{ if } k = g(l) \\ \qquad\qquad k = 1, \ldots, d \text{ and } l = 1, \ldots, [r_3 \cdot d] \\ 0 \text{ else} \end{cases} \tag{6}$$

$$g = r \text{ and } perm(d) \tag{7}$$

$$n_1 \sim N(0, 1) \tag{8}$$

where r_1, r_2, and r_3 denotes three random integers between (0, 1), $\vec{p}_i(t+1)$ shows the candidate's location of i-th rabbits at $t+1$ time, L shows the movement pace of rabbit, $\vec{\chi}_i$ indicates the $i-th$ location of rabbit at t time , n denotes the population

size of the rabbit, d denotes the number of variables in the problems that should be enhanced, n_1 is subjected to the uniform distribution, and T indicates the maximal iterations. R characterizes the running operator that mimics rabbits' running characteristics indicating the mapping vector.

3) RANDOM HIDING (EXPLOITATION)

Every rabbit has d burrow near the nest to randomly choose one of them to hide in and escape from predators.

$$\vec{b}(t) = \vec{x}(t) + H \times g \times \vec{x}(t), i = 1, \ldots, n \text{ and } j = 1, \ldots, d \quad (9)$$

$$H = \frac{T - t + 1}{T} \times r_4 \quad (10)$$

$$g(k) = \begin{cases} 1 \text{ if } k = j \\ 0 \text{ else} \end{cases} \quad k = 1, \ldots, d \quad (11)$$

$$\vec{p}_i(t+1) = \vec{\chi}_i + R \times (r_4 \times \vec{b}_{i,r}(t) - \vec{\chi}_i = 1, \ldots, n \quad (12)$$

$$g_r(k) = \begin{cases} 1 \text{ if } k = [r_5 \times d] \\ 0 \text{ else} \end{cases} \quad k = 1, \ldots, d \quad (13)$$

$$\vec{b}_{i,r}(t) = \vec{x}_i(t) + H \times g_r \times \vec{x}_i(t), i = 1, \ldots, n \quad (14)$$

$$\vec{x}(t+1) = \begin{cases} \vec{\chi}_i \le f(\vec{p}_i(t+1)) \\ \vec{p}_i(t+1) f(\vec{x}_i(t)) > f(\vec{p}_i(t+1)) \end{cases} \quad (15)$$

where $\vec{b}_{i,j}$ shows the jth burrow for the ith rabbit, H refers to the hiding parameter, $\vec{b}_{i,r}$ represent the burrow chosen randomly for hiding for the ith rabbit, demonstrated in Eq. (14), and r_4 and r_5 represent the random number within (0, 1).

Eq. (12) denotes that the ith rabbit attempts to change the location based on the randomly chosen burrow. Finally, in random hiding or detour foraging, the rabbit leaves the existing location and persists at the candidate location once the fitness of the candidate's location of ith rabbit is better than the preceding one, as demonstrated in Eq. (15).

In this method, a present weight finds all objective significance by integrating the objectives into a single objective formula [25]. Here, a fitness function (FF) is applied, which merges both objectives of FS as exposed in (16).

$$Fitness(X) = \alpha \cdot E(X) + \beta * \left(1 - \frac{|R|}{|N|}\right) \quad (16)$$

Here, $|N|$ and $|R|$ is the count of original features and the count of selected features in the dataset; Fitness (X) refers to the fitness value of subset X, β and α indicate the weights of the reduction ratio and classifier error, $\alpha \in [0, 1]$ and $\beta = (1 - \alpha)$, $E(X)$ signifies the classifier error rate utilizing the chosen features in the X subset.

C. MEDICAL DATA CLASSIFICATION USING CSCR-ELM MODEL

In this work, the CSCR-ELM method is utilized for medical data classification. The input bias and weight of SLFN are created randomly [26]. An equivalent output matrix of hidden state was calculated concerning the output weighted with some steps. Thus, the computational cost of ELM was lesser. Fig. 2 defines the structure of ELM. Consider that there are N instances determined by $(X_i, y_i), i = 1, 2, \ldots, N$. $X_i = [x_{i1}, x_{i2}, \ldots, x_{in}]^T 2R^n$ and $y_i = [y_{i1}, y_{i2}, \ldots, y_{im}]^T 2R^m$. Consider a_j and β_j correspondingly as input and output weighted. b_j denotes the bias of hidden units. The SLFN having L hidden node is modelled by Eq. (17):

$$\sum_{j=1}^{L} \beta_j g(a_j, b_j, X_i) = 0_i, i = 1, \ldots, N \quad (17)$$

where $g(\bullet)$ indicates the activation function and usually exploits nonlinear functions such as radial sine, basis function, sigmoid, and so on. The error amongst estimated output 0_i and the actual output y_i is zero if the SLFN exactly evaluate the data feature.

$$\sum_{j=1}^{L} \beta_j g(a_j, b_j, X_i) = y_i, i = 1, \ldots, N \quad (18)$$

Consider $\beta = [\beta_1^T, \ldots, \beta_L^T]^T$ and $Y = [y_{1^T}, \ldots, y_{N^T}]^T$. The abovementioned technique is denoted by $H\beta = Y$.

$$H = \begin{bmatrix} g(a_1, b_1, X_1) & \ldots & g(a_L, b_L, X_1) \\ \vdots & \ldots & \vdots \\ g(a_1, b_1, X_N) & \ldots & g(a_L, b_L, X_N) \end{bmatrix} \quad (19)$$

In Eq. (19), H indicates the supposed output matrix of the hidden state. h_{ij} shows the output of j^{th} hidden node corresponding to input X_i. In the trained procedure, the parameter of hidden nodes encompassing a_j and b_j couldn't be adapted then primarily constructed. Equal output weighted is estimated by:

$$\widehat{\beta} = \mathrm{H}^{\dagger} Y = \begin{cases} (\frac{l}{c} + H^T H)^{-1} H^T Y, L < N \\ H^T (\frac{l}{c} + H^T H)^{-1} Y, L \ge N \end{cases} \quad (20)$$

In Eq. (20), $\mathrm{H}^{\dagger}$ indicates Moore-Penrose generalization inverse of H. C represents the present parameter, intends to provide trade-offs between minimalizing the trained error and maximizing marginal distance. I represent the unit matrix. The best output weighted is attained by minimalising the cost function $\| O - Y \|$.

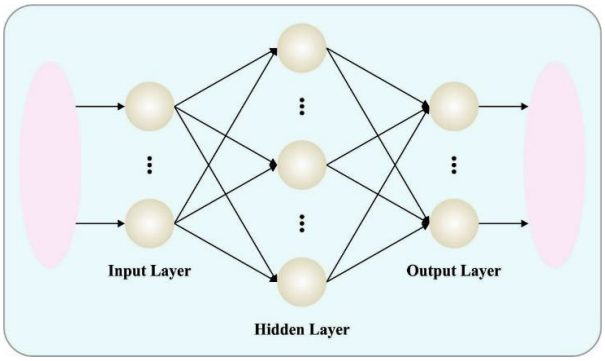

FIGURE 2. Architecture of ELM.

After establishing class-specific regulation costs, CCR-ELM was projected to resolve the class imbalance issue. The 2 trade-off factors encompassing C^+ for minority positive instances and C^- for most negative instances are exploited to rebalance both classes. Consider the amount of minority positive instances and majority negative instances formulated by l_1 and l_2 correspondingly. CCR-ELM was modelled by Eq. (21):

$$\min\left(\frac{1}{2}\|\beta\|^2 + \frac{1}{2}C^+ \sum_{i=1|y_{i=+1}}^{l_1} \xi_i^2 + \frac{1}{2}C^- \sum_{i=1|y_{i=-1}}^{l_2} \xi_i^2\right)$$
$$s.t.\ h(x_i)\beta = y_i - \xi_i, i\mathcal{D}\ 1, \ldots N. \tag{21}$$

Correspondent output weighted $\widehat{\beta}$ is evaluated by:

$$\widehat{\beta} = H^{\dagger}Y = \begin{cases} (\frac{I}{C^+} + \frac{I}{C^-} + H^T H)^{-1} H^T Y, L < N \\ H^T (\frac{1}{C^+} + \frac{I}{C^-} + H^T H)^{-1} Y, L \geq N \end{cases} \tag{22}$$

To binary classifier issues, the decision function of the CCR-ELM-based classifier was $f(x) = signh(x)\beta$.

$$f(x) = \begin{cases} sign\ h(x)(\frac{I}{C^+} + \frac{I}{C^-} + H^T H)^{-1} H^T Y, L < N \\ sign\ h(x) H^T (\frac{I}{C^+} + \frac{I}{C^-} + H^T H)^{-1} Y, L \geq N \end{cases} \tag{23}$$

In CCR-ELM, 5 key parameters have direct feature on the classifier performance, including the amount of hidden nodes L, biases b_j, C^+ for minority positive instances, input weighted a_j, and C^- for most negative instances. The previous 3 variables define the architecture of SLFN and usually was present by humans.

D. PARAMETER TUNING USING GOA

Lastly, the GOA optimally selects the parameters related to the CSCR-ELM model. The grasshopper is a beetle. Because of the harm it causes to crop and agriculture production, it can be assumed to be a pest [27]. The two significant stages in the life cycle of a grasshopper are adult and larva. The equations define the mathematical methods exploited to simulate grasshopper movement:

$$X_i = S_i + G_i + A_i \tag{24}$$
$$S_i = \sum_{j=1, j\neq i}^{N} s\left(d_{ij}\right) \widehat{d}_{ij} \tag{25}$$
$$s\left(r\right) = fe^{-\frac{r}{l}} - e^{-r} \tag{26}$$
$$\text{E}.G_i = -g\widehat{e_g} \tag{27}$$
$$A_i = u\widehat{e_w} \tag{28}$$

Here X_i, G_i, A_i, and S_i indicate the grasshopper position, gravitational force, wind advection and social interaction forces, $\widehat{d_i}$,d and did denote the unit vector and distance from the ith to the *jth* grasshopper, where f intensity of attraction and l means the attractive length scale , $s(r)$ refers to a social force among two grasshoppers. In Eq. (27), $\widehat{e}$.g. means the unity vector toward the earth's centre, and g is the gravitational constant. In Eq. (28), $\widehat{e_w}$ denotes unity vectors in the wind direction, and u is a constant drift. An altered version of the equation to resolve optimization issues was expressed below:

$$X_i^d = c\left(\sum_{j=1,j\neq 1}^{N} c\frac{ub_d - lb_d}{2} s(|x_j^d - x_i^d|)\frac{\chi_{j-\chi i}}{d_{ij}}\right) + \widehat{T_d} \tag{29}$$

Here ub_d and lb_d are the upper and lower bounds in the dth dimension, c was a diminishing coefficient to shrink the comfort, repulsion and attraction area, and $\widehat{T_d}$ signifies the dth dimension value in target. The formula utilized to update the parameter c is as follows:

$$c = c_{\max} - i\frac{c_{\max} - c_{\min}}{L} \tag{30}$$

where $c_{\max}$ denotes the maximal value, $c_{\min}$ indicates the minimal value, i is the index for the current iteration, and L implies maximal iterations.

The GOA method derived a FF to reach enriched classifier performance. It determined a positive integer to denote the superior outcome of candidate solutions. The minimalized classifier error rate was the FF, as Eq. (31) specified.

$$fitness\ (x_i) = \frac{No.\ of\ misclassified\ samples}{Total\ No.\ of\ samples} * 100 \tag{31}$$

IV. EXPERIMENTAL VALIDATION

In this study, the experimental result analysis of the AROML-HDC technique is examined on two medical datasets: the Cleveland dataset [28] and the Statlog dataset [29]. Here, the Cleveland dataset includes 297 samples, and the Statlog dataset comprises 270 samples, as represented in Table 1. The attributes involved in Cleveland dataset are age, sex, chest pain, resting blood pressure, cholesterol, fasting blood sugar, resting electrocardiographic results, predicted attribute, thal, number of major vessels, slope, old peak, exercise induced angina, and maximum heart rate achieved. The Statlog dataset has 13 attributes such as age, sex, chest pain, resting blood pressure, serum cholesterol, fasting blood sugar, resting electrocardiographic results, maximum heart rate achieved, exercise induced angina, old peak, slope of the peak exercise ST segment, number of major vessels (0-3) colored by flourosopy, and thal.

A set of measures used to examine the classification results are accuracy ($accu_y$), precision ($prec_n$), recall ($reca_l$), and F-score (F_{score}).

TABLE 1. Details of the dataset.

Class	No. of Instances	
	Cleveland Dataset	Statlog Dataset
Absence	160	150
Presence	137	120
Total No. of Instances	**297**	**270**

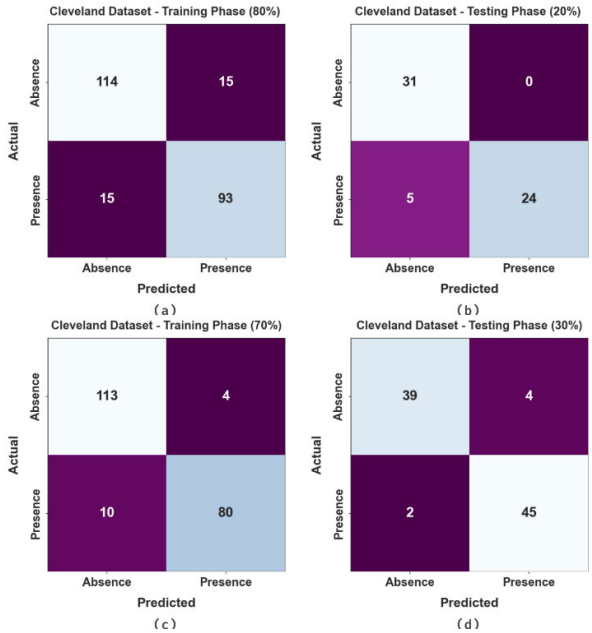

FIGURE 3. Confusion matrices of AROML-HDC technique on Cleveland dataset (a-b) 80:20 of TRP/TSP and (c-d) 70:30 of TRP/TSP.

Precision measures the proportion of correctly predicted positive instances out of all the instances that were predicted as positive.

$$\text{Precision} = \frac{\text{TP}}{\text{TP} + \text{FP}} \tag{32}$$

Recall measures the proportion of positive samples correctly classified.

$$\text{Recall} = \frac{\text{TP}}{\text{TP} + \text{FN}} \tag{33}$$

Accuracy measures the proportion of correctly classified samples (positives and negatives) against the total samples (number of samples that have been classified).

$$\text{Accuracy} = \frac{\text{TP} + \text{TN}}{\text{TP} + \text{TN} + \text{FP} + \text{FN}} \tag{34}$$

F-score is a measure combining the harmonic mean of precision and recall.

$$\text{F} - \text{score} = \frac{2\text{TP}}{2\text{TP} + \text{FP} + \text{FN}} \tag{35}$$

The confusion matrices of the AROML-HDC technique on the Cleveland dataset are revealed in Fig. 3. On 80% of TRP, the AROML-HDC technique recognizes 114 absence samples and 93 presence samples. Next, on 20% of TSP, the AROML-HDC approach recognizes 31 absence samples and 24 presence samples. Along with that, on 70% of TRP, the AROML-HDC technique recognizes 113 absence samples and 80 presence samples. Finally, on 30% of TSP, the AROML-HDC algorithm recognizes 39 absence samples and 45 presence samples.

In Table 2 and Fig. 4, the overall outcomes of the AROML-HDC approach on the Cleveland dataset are exhibited.

TABLE 2. Classification outcome of AROML-HDC approach on cleveland dataset.

Class	$Accu_y$	$Prec_n$	$Reca_l$	F_{score}	MCC
Training Phase (80%)					
Absence	88.37	88.37	88.37	88.37	74.48
Presence	86.11	86.11	86.11	86.11	74.48
Average	**87.24**	**87.24**	**87.24**	**87.24**	**74.48**
Testing Phase (20%)					
Absence	100.00	86.11	100.00	92.54	84.42
Presence	82.76	100.00	82.76	90.57	84.42
Average	**91.38**	**93.06**	**91.38**	**91.55**	**84.42**
Training Phase (70%)					
Absence	96.58	91.87	96.58	94.17	86.29
Presence	88.89	95.24	88.89	91.95	86.29
Average	**92.74**	**93.55**	**92.74**	**93.06**	**86.29**
Testing Phase (30%)					
Absence	90.70	95.12	90.70	92.86	86.70
Presence	95.74	91.84	95.74	93.75	86.70
Average	**93.22**	**93.48**	**93.22**	**93.30**	**86.70**

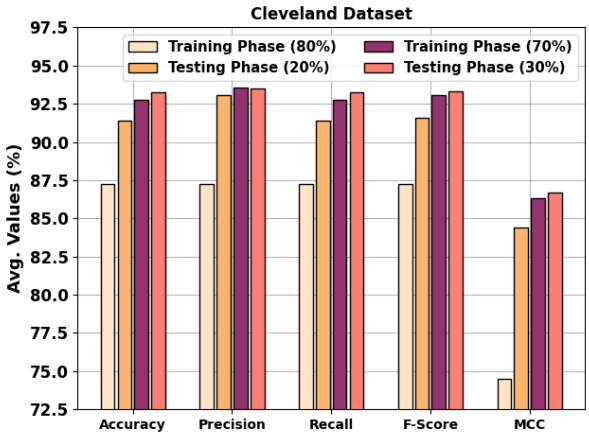

FIGURE 4. Average outcome of AROML-HDC approach on Cleveland dataset.

The outcomes indicate the effectual identification of the absence and presence of class samples. For instance, with 80% of TRP, the AROML-HDC approach reaches average $accu_y$ of 87.24%, $prec_n$ of 87.24%, $reca_l$ of 87.24%, F_{score} of 87.24%, and MCC of 74.48%. Besides, with 20% of TSP, the AROML-HDC technique reaches average $accu_y$ of 91.38%, $prec_n$ of 93.06%, $reca_l$ of 91.38%, F_{score} of 91.55%, and MCC of 84.42%. Also, with 70% of TRP, the AROML-HDC technique reaches average $accu_y$ of 92.74%, $prec_n$ of 93.55%, $reca_l$ of 92.74%, F_{score} of 93.06%, and MCC of 86.29%.

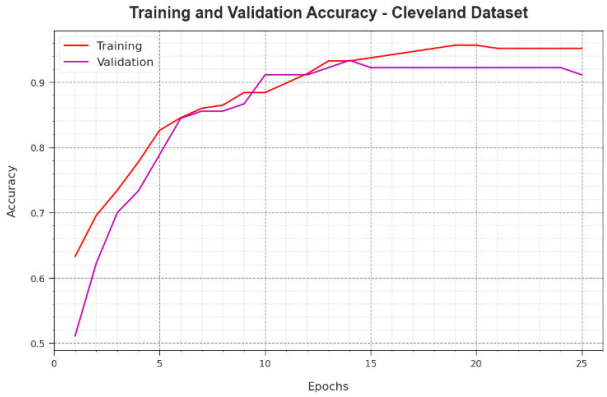

FIGURE 5. Accuracy curve of AROML-HDC approach on Cleveland dataset.

Fig. 5 examines the accuracy of the AROML-HDC method during the training and validation process on the Cleveland dataset. The figure specifies that the AROML-HDC approach reaches increasing accuracy values over increasing epochs. Further, the increasing validation accuracy over training accuracy exhibits that the AROML-HDC method learns efficiently on the Cleveland dataset.

The loss analysis of the AROML-HDC technique at the time of training and validation is demonstrated on the Cleveland dataset in Fig. 6. The results indicate that the AROML-HDC technique reaches closer values of training and validation loss. The AROML-HDC technique learns efficiently on the Cleveland dataset.

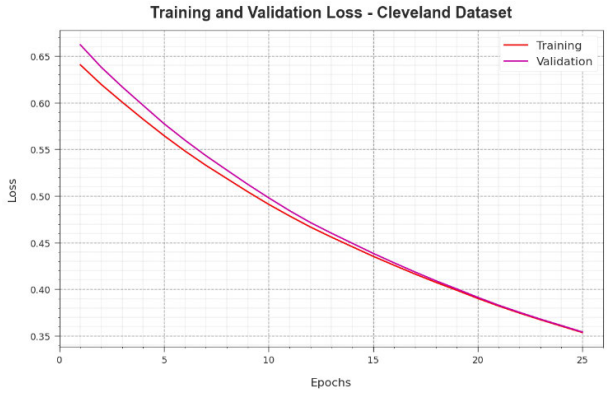

FIGURE 6. Loss curve of AROML-HDC approach on Cleveland dataset.

The confusion matrices of the AROML-HDC technique on the Statlog dataset are revealed in Fig. 7. On 80% of TRP, the AROML-HDC approach recognizes 107 absence samples and 96 presence samples. Next, on 20% of TSP, the AROML-HDC technique recognizes 32 absence samples and 18 presence samples. In addition, on 70% of TRP, the AROML-HDC technique recognizes 98 absence samples and 74 presence samples. Eventually, on 30% of TSP, the AROML-HDC method recognizes 52 absence samples and 24 presence samples.

In Table 3 and Fig. 8, the overall results of the AROML-HDC system on the Statlog dataset are exhibited. The figure

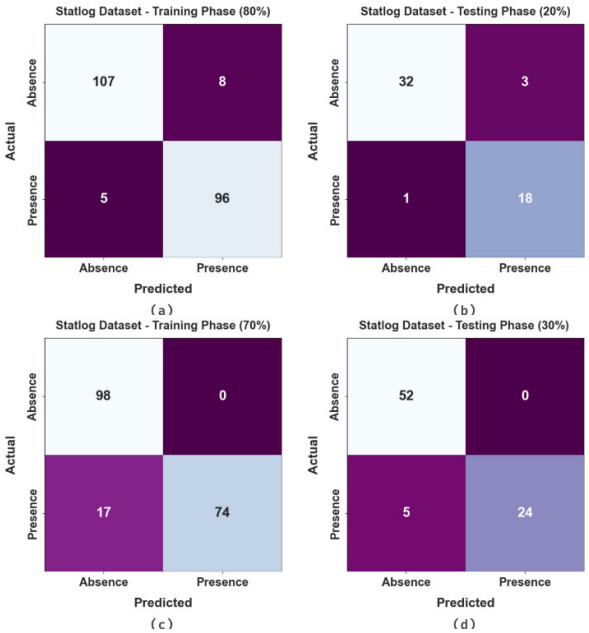

FIGURE 7. Confusion matrices of AROML-HDC technique on Statlog dataset (a-b) 80:20 of TRP/TSP and (c-d) 70:30 of TRP/TSP.

TABLE 3. Classification outcome of AROML-HDC method on statlog dataset.

Statlog Dataset					
Class	$Accu_y$	$Prec_n$	$Reca_l$	F_{score}	MCC
Training Phase (80%)					
Absence	93.04	95.54	93.04	94.27	87.97
Presence	95.05	92.31	95.05	93.66	87.97
Average	**94.05**	**93.92**	**94.05**	**93.97**	**87.97**
Testing Phase (20%)					
Absence	91.43	96.97	91.43	94.12	84.41
Presence	94.74	85.71	94.74	90.00	84.41
Average	**93.08**	**91.34**	**93.08**	**92.06**	**84.41**
Training Phase (70%)					
Absence	100.00	85.22	100.00	92.02	83.25
Presence	81.32	100.00	81.32	89.70	83.25
Average	**90.66**	**92.61**	**90.66**	**90.86**	**83.25**
Testing Phase (30%)					
Absence	100.00	91.23	100.00	95.41	86.89
Presence	82.76	100.00	82.76	90.57	86.89
Average	**91.38**	**95.61**	**91.38**	**92.99**	**86.89**

indicates the effectual identification of the absence and presence of class samples. For instance, with 80% of TRP, the AROML-HDC approach reaches an average $accu_y$ of 94.05%, $prec_n$ of 93.92%, $reca_l$ of 94.05%, F_{score} of 93.97%, and MCC of 87.97%. Besides, with 20% of TSP, the AROML-HDC method reaches average $accu_y$ of 93.08%, $prec_n$ of 91.34%, $reca_l$ of 93.08%, F_{score} of 92.06%, and MCC of 84.41%. Also, with 70% of TRP, the AROML-HDC method reaches average $accu_y$ of 90.66%, $prec_n$ of 92.61%, $reca_l$ of 90.66%, F_{score} of 90.86%, and MCC of 83.25%.

Fig. 9 examines the accuracy of the AROML-HDC technique during the training and validation process on the Statlog dataset. The figure notifies that the AROML-HDC technique reaches increasing accuracy values over increasing epochs.

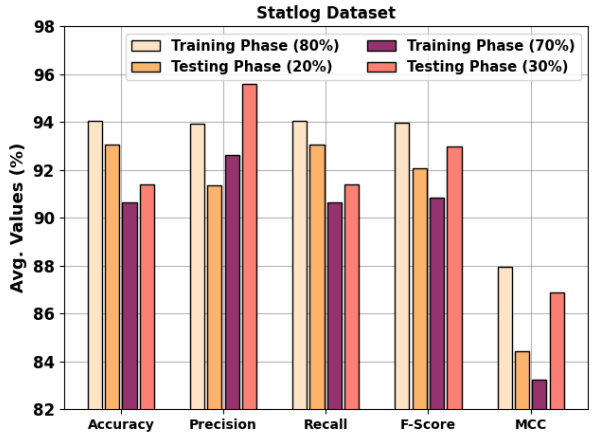

FIGURE 8. Average outcome of AROML-HDC approach on Statlog dataset.

FIGURE 9. Accuracy curve of AROML-HDC approach on Statlog dataset.

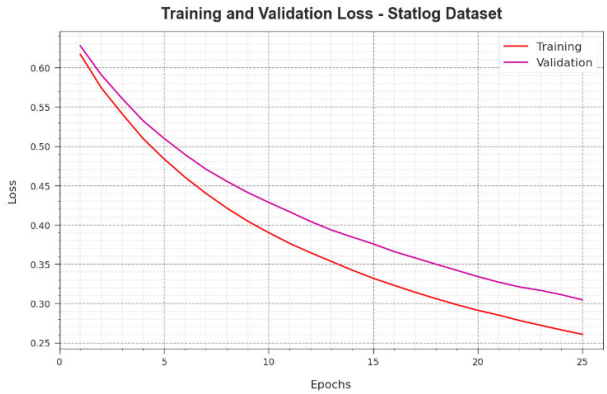

FIGURE 10. Loss curve of AROML-HDC approach on Statlog dataset.

In addition, the increasing validation accuracy over training accuracy exhibits that the AROML-HDC technique learns efficiently on Statlog dataset.

The loss analysis of the AROML-HDC technique at the time of training and validation is demonstrated on Statlog dataset in Fig. 10. The results indicate that the AROML-HDC technique reaches closer values of training and validation loss. The AROML-HDC technique learns efficiently on Statlog dataset.

TABLE 4. Accuracy outcome of AROML-HDC approach with other existing methods.

Methods	Accuracy (%)
AROML-HDC	94.05
MLMDMC-ED	91.87
VNB-LR	87.71
Fuzzy-NN	80.36
DT	81.04
ELM	86.87
SVM	86.42
NB	69.31
CART	83.23
GA-NN	80.9
DT-GR	84.49

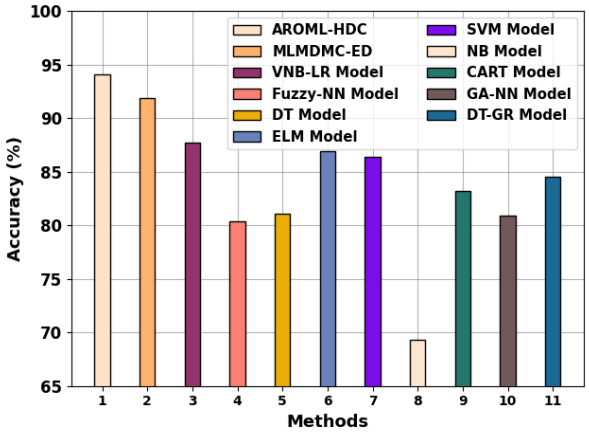

FIGURE 11. Accuracy outcome of AROML-HDC method with other existing methods.

At the last stage, the betterment of the AROML-HDC technique is confirmed by performing a comparison study in terms of $accu_y$ in Table 4 and Fig. 11 [30]. These results represent the improved efficacy of the AROML-HDC method with an increasing $accu_y$ of 94.05%.

On the other hand, the MLMDMC-ED, VNB-LR, fuzzy-NN, DT, ELM, SVM, NB, CART, GA-NN, and DT-GR methods accomplished reduced performance with $accu_y$ of 91.87%, 87.71%, 80.36%, 81.04%, 86.87%, 86.42%, 69.31%, 83.23%, 80.9%, and 84.49% respectively. Therefore, the AROML-HDC technique can be applied for effective healthcare data analysis in the ED of the KSA hospitals.

V. CONCLUSION

In this study, we have introduced a new AROML-HDC technique for classifying and monitoring medical data in the ED of the KSA hospitals. The presented AROML-HDC

technique monitors and tracks the patient visit data, treatment given, and LOS. In addition, the AROML-HDC technique performs medical data classification via different sub-processes namely min-max normalization, ARO-based feature subset selection, CSCR-ELM classification, and GOA-based parameter tuning. The design of the ARO algorithm and GOA helps to intensify the overall performance of the AROML-HDC technique in the medical data classification process. The experimental outcomes of the AROML-HDC technique were tested on a benchmark healthcare dataset, and the results indicate the improved performance of the AROML-HDC methodology with other recent methods in terms of different measures. In the upcoming years, the presented AROML-HDC technique can be extended to the design of a fusion-based ensemble classifier to improvise the classification performance.

REFERENCES

[1] B. Godi, S. Viswanadham, A. S. Muttipati, O. P. Samantray, and S. R. Gadiraju, "E-healthcare monitoring system using IoT with machine learning approaches," in *Proc. Int. Conf. Comput. Sci., Eng. Appl.*, Mar. 2020, pp. 1–5.

[2] T. M. Ghazal, M. K. Hasan, M. T. Alshurideh, H. M. Alzoubi, M. Ahmad, S. S. Akbar, B. Al Kurdi, and I. A. Akour, "IoT for smart cities: Machine learning approaches in smart healthcare—A review," *Future Internet*, vol. 13, no. 8, p. 218, Aug. 2021.

[3] A. Gupta and R. Katarya, "Social media based surveillance systems for healthcare using machine learning: A systematic review," *J. Biomed. Informat.*, vol. 108, Aug. 2020, Art. no. 103500.

[4] K. Muhammad, S. Khan, J. D. Ser, and V. H. C. D. Albuquerque, "Deep learning for multigrade brain tumor classification in smart healthcare systems: A prospective survey," *IEEE Trans. Neural Netw. Learn. Syst.*, vol. 32, no. 2, pp. 507–522, Feb. 2021.

[5] Z. Ahmed, K. Mohamed, S. Zeeshan, and X. Dong, "Artificial intelligence with multi-functional machine learning platform development for better healthcare and precision medicine," *Database*, vol. 2020, Jan. 2020.

[6] W. Li, Y. Chai, F. Khan, S. R. U. Jan, S. Verma, V. G. Menon, and X. Li, "A comprehensive survey on machine learning-based big data analytics for IoT-enabled smart healthcare system," *Mobile Netw. Appl.*, vol. 26, no. 1, pp. 234–252, Feb. 2021.

[7] H. K. Bharadwaj, A. Agarwal, V. Chamola, N. R. Lakkaniga, V. Hassija, M. Guizani, and B. Sikdar, "A review on the role of machine learning in enabling IoT based healthcare applications," *IEEE Access*, vol. 9, pp. 38859–38890, 2021.

[8] S. Durga, R. Nag, and E. Daniel, "Survey on machine learning and deep learning algorithms used in Internet of Things (IoT) healthcare," in *Proc. 3rd Int. Conf. Comput. Methodologies Commun. (ICCMC)*, Mar. 2019, pp. 1018–1022.

[9] U. M. Butt, S. Letchmunan, M. Ali, F. H. Hassan, A. Baqir, and H. H. R. Sherazi, "Machine learning based diabetes classification and prediction for healthcare applications," *J. Healthcare Eng.*, vol. 2021, pp. 1–17, Sep. 2021.

[10] L. Tan, K. Yu, A. K. Bashir, X. Cheng, F. Ming, L. Zhao, and X. Zhou, "Toward real-time and efficient cardiovascular monitoring for COVID-19 patients by 5G-enabled wearable medical devices: A deep learning approach," *Neural Comput. Appl.*, vol. 2021, pp. 1–14, Jan. 2021.

[11] A. Kishor and C. Chakraborty, "Artificial intelligence and Internet of Things based healthcare 4.0 monitoring system," *Wireless Pers. Commun.*, vol. 127, no. 2, pp. 1615–1631, Nov. 2022.

[12] A. Kishor, C. Chakraborty, and W. Jeberson, "A novel fog computing approach for minimization of latency in healthcare using machine learning," *Int. J. Interact. Multimedia Artif. Intell.*, vol. 6, no. 7, p. 7, 2021.

[13] F. Ali, S. El-Sappagh, S. M. R. Islam, A. Ali, M. Attique, M. Imran, and K.-S. Kwak, "An intelligent healthcare monitoring framework using wearable sensors and social networking data," *Future Gener. Comput. Syst.*, vol. 114, pp. 23–43, Jan. 2021.

[14] A. Souri, M. Y. Ghafour, A. M. Ahmed, F. Safara, A. Yamini, and M. Hoseyninezhad, "A new machine learning-based healthcare monitoring model for student's condition diagnosis in Internet of Things environment," *Soft Comput.*, vol. 24, no. 22, pp. 17111–17121, Nov. 2020.

[15] N. Surantha, T. F. Lesmana, and S. M. Isa, "Sleep stage classification using extreme learning machine and particle swarm optimization for healthcare big data," *J. Big Data*, vol. 8, no. 1, pp. 1–17, Dec. 2021.

[16] K. Harimoorthy and M. Thangavelu, "Multi-disease prediction model using improved SVM-radial bias technique in healthcare monitoring system," *J. Ambient Intell. Humanized Comput.*, vol. 12, no. 3, pp. 3715–3723, Mar. 2021.

[17] P. Kaur, R. Kumar, and M. Kumar, "A healthcare monitoring system using random forest and Internet of Things (IoT)," *Multimedia Tools Appl.*, vol. 78, no. 14, pp. 19905–19916, Jul. 2019.

[18] J. J. Oskvarek, M. S. Zocchi, A. Cai, A. Venkat, A. T. Janke, A. Venkatesh, and J. M. Pines, "Development and internal validation of an emergency department admission intensity measure using data from a national group," *Ann. Emergency Med.*, vol. 2023, pp. 1–23, Jan. 2023.

[19] F. Kadri, A. Dairi, F. Harrou, and Y. Sun, "Towards accurate prediction of patient length of stay at emergency department: A GAN-driven deep learning framework," *J. Ambient Intell. Humanized Comput.*, vol. 2022, pp. 1–15, Feb. 2022.

[20] D. Kavitha and S. Ravikumar, "IOTand context-aware learning-based optimal neural network model for real-time health monitoring," *Trans. Emerg. Telecommun. Technol.*, vol. 32, no. 1, pp. 1–13, Jan. 2021.

[21] T. Goto, C. A. Camargo, M. K. Faridi, R. J. Freishtat, and K. Hasegawa, "Machine learning-based prediction of clinical outcomes for children during emergency department triage," *JAMA Netw. Open*, vol. 2, no. 1, Jan. 2019, Art. no. e186937.

[22] L. D. Nymoen, M. Björk, T. E. Flatebø, M. Nilsen, A. Godø, E. Øie, and K. K. Viktil, "Drug-related emergency department visits: Prevalence and risk factors," *Internal Emergency Med.*, vol. 17, no. 5, pp. 1453–1462, Aug. 2022.

[23] W. Xu and R. S. Cloutier, "A facial expression recognizer using modified ResNet-152," *EAI Endorsed Trans. Internet Things*, vol. 7, no. 28, p. e5, Apr. 2022.

[24] A. J. Riad, H. M. Hasanien, R. A. Turky, and A. H. Yakout, "Identifying the PEM fuel cell parameters using artificial rabbits optimization algorithm," *Sustainability*, vol. 15, no. 5, p. 4625, Mar. 2023.

[25] M. Mafarja, T. Thaher, M. A. Al-Betar, J. Too, M. A. Awadallah, I. A. Doush, and H. Turabieh, "Classification framework for faulty-software using enhanced exploratory whale optimizer-based feature selection scheme and random forest ensemble learning," *Int. J. Speech Technol.*, vol. 2023, pp. 1–43, Feb. 2023.

[26] J. Cheng, J. Chen, Y.-N. Guo, S. Cheng, L. Yang, and P. Zhang, "Adaptive CCR-ELM with variable-length brain storm optimization algorithm for class-imbalance learning," *Natural Comput.*, vol. 20, no. 1, pp. 11–22, Mar. 2021.

[27] A. Sherif and H. Haci, "A novel bio-inspired energy optimization for two-tier wireless communication networks: A grasshopper optimization algorithm (GOA)-based approach," *Electronics*, vol. 12, no. 5, p. 1216, Mar. 2023.

[28] W. A. David. (1988). *Heart Disease Data Set*. [Online]. Available: https://archive.ics.uci.edu/ml/datasets/heart+disease

[29] Accessed: Feb. 12, 2023. [Online]. Available: https://archive.ics.uci.edu/ml/datasets/statlog+(heart)

[30] M. Ragab, F. Kateb, M. W. Al-Rabia, D. Hamed, T. Althaqafi, and A. S. A.-M. Al-Ghamdi, "A machine learning approach for monitoring and classifying healthcare data—A case of emergency department of KSA hospitals," *Int. J. Environ. Res. Public Health*, vol. 20, no. 6, p. 4794, Mar. 2023, doi: 10.3390/ijerph20064794.